EurJOC
European Journal of Organic Chemistry

Research Article
doi.org/10.1002/ejoc.202200204

Chemistry Europe
European Chemical Societies Publishing

www.eurjoc.org

Very Important Paper

Base-Mediated Remote Deuteration of *N*-Heteroarenes – Broad Scope and Mechanism

Sara Kopf,[a] Jiali Liu,[a, b, c] Robert Franke,[b, c] Haijun Jiao,*[a] Helfried Neumann,*[a] and Matthias Beller*[a]

Deuterated organic molecules provide the basis for many applications in life sciences and material research. Thus, methodologies to access labeled compounds with defined selectivity continue to be important. Using KO*t*Bu as base and DMSO-d_6 as deuterium source, we present a general and applicable method for the selective deuteration of a set of nitrogen-containing heterocycles (pyridines, azines and bioactive molecules). Experimental and DFT mechanistic studies indicate that this reaction proceeds *via* deprotonation of the substrates by the dimsyl anion. The relative thermodynamic stability of the heterocycle anions determines the distribution and degree of deuteration.

Introduction

Kinetic isotope effects stemming from the replacement of the lightest isotope of hydrogen, protium, by its heavier congeners, deuterium and tritium, is a common concept in physical organic chemistry for mechanistic studies of many organic transformations.[1] The profound mass difference of the isotopes of hydrogen results in a measurably lower zero-point energy for C–D bonds compared to C–H bonds, leading to higher activation barriers;[1c] and the comparative measurement of reaction rates for substrates containing C–H and C–D bonds is an important tool to probe the participation of the C–H bond cleavage step in mechanisms of organic reactions.[1] The significant difference in stability and activity between C–H and C–D bonds provides the basis for applications in life sciences where the selective replacement of protium by deuterium at specific, metabolically labile, sites in a drug molecule can enhance the pharmacokinetic properties such as metabolic stability.[2] Successfully employing this approach, the first deuterated drug, Austedo (deutetrabenazine), was launched in 2017 and currently more deuterated drug candidates are in clinic trials.[2] While this application requires chemical reactions that enable selective installation of deuterium atoms in drug scaffolds, methodologies that drive the incorporation of several deuterium atoms at once are highly sought after for the preparation of stable isotopically labeled internal standards for mass spectrometric bioanalytics.[1e,2a,3]

In this context, reactions targeting structural moieties common in bioactive compounds are especially useful. Being the second most common nitrogen heterocycle and the most common nitrogen-containing aromatic heterocycle in drugs approved by the federal drug administration in the US (FDA) as of 2014, pyridines appear to be particularly attractive substrates for deuteration reactions.[4] Their further use as ligands in material science[5] and homogeneous catalysis[6] may open up more possible applications for deuterated compounds.[7,8] It is therefore not surprising that methodologies for the deuteration of pyridines have been developed as early as in the 1960s.[9]

For the selective deuterium installation in specific positions of pyridines, prefunctionalized substrates, such as pyridine carboxylic acids or halogenated pyridines, have been used in deuterodehalogenation[9b,10] and other reductive deuteration reactions.[9e] Similarly, directed lithiation with subsequent hydrolysis can afford good selectivity.[11] However, the former reaction may suffer from less accessible substrates and selectivity problems in the prefunctionalization step, while the latter requires harsh reaction conditions, impeding the use for late stage deuteration of sensitive substrates. Therefore, methodologies allowing for the direct exchange of a hydrogen atom for a deuterium atom in one step (hydrogen isotope exchange, HIE) at a late stage are more desirable.[1e,3] While the moiety of pyridine has been famously used as a directing group for the iridium-catalyzed HIE in the *ortho* positions of adjacent aromatic rings (Scheme 1)[12] and the increased reactivity of benzylic positions at pyridine rings can be exploited for acid-catalyzed HIE,[13] more drastic conditions such as heating the substrate in a solution of NaOD in supercritical D_2O can enable complete deuteration of all positions in a pyridine ring (Scheme 1).[14] Heterogeneous[15] and homogeneous[16] noble metal catalysts facilitate this transformation under milder conditions. However, the selective deuteration of positions

[a] S. Kopf, J. Liu, Dr. H. Jiao, Dr. H. Neumann, Prof. Dr. M. Beller
Leibniz-Institut für Katalyse e. V., Rostock
Albert-Einstein-Straße 29a, 18059 Rostock, Germany
E-mail: Helfried.Neumann@catalysis.de
Haijun.Jiao@catalysis.de
Matthias.Beller@catalysis.de
www.catalysis.de
[b] J. Liu, Prof. Dr. R. Franke
Evonik Operations GmbH
Paul-Baumann-Straße 1, 45772 Marl, Germany
[c] J. Liu, Prof. Dr. R. Franke
Lehrstuhl für Theoretische Chemie
Ruhr-Universität Bochum, 44780 Bochum, Germany

Supporting information for this article is available on the WWW under https://doi.org/10.1002/ejoc.202200204

Research Article
doi.org/10.1002/ejoc.202200204

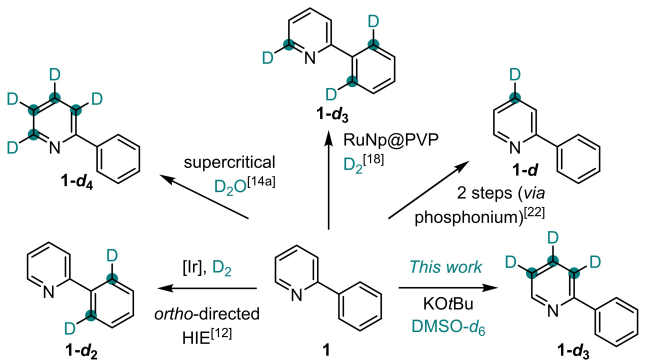

Scheme 1. Selectivity patterns accessed with various HIE methodologies for the labeling of 2-phenylpyridine.

proximal to the heteroatom has been observed more often when using heterogeneous catalysts[17] and especially good results under milder conditions have been achieved with ruthenium nanoparticles (Scheme 1).[18] In this case, the observed selectivity results from the directing effect of the nitrogen atom when coordinated to the metal surface.[18] On the other hand, when homogeneous catalysts are sufficiently tuned to preferentially undergo C–H activation in electron-rich positions, similar results have been achieved.[19]

To allow for a broad range of labeling possibilities, it is desirable to have a toolkit that can access various selectivity patterns in the deuteration of pyridines. To this end, interesting approaches have been the combination of homogeneous and heterogeneous catalysts to combine their respective selectivities,[20] the use of catalysts that exhibit a purely sterically driven selectivity[21] as well as the implementation of a two-step protocol that enables selective deuteration in position 4 of pyridines (Scheme 1).[22] On the other hand, a preference for the distal positions of pyridine derivatives was observed in kinetic experiments with osmium complexes[23] as well as with NaOD.[24] These reports arose our interest in remote labeling strategies, leading to the development of a methodology for the HIE of distal positions in pyridine derivatives with the aim to complement the existing labeling strategies for this substrate class. It should be noted that during the preparation of this manuscript, a related study on the deuteration of pyridines was published.[25] Herein, we report our work including a complementary scope and additional mechanistic insights based on experiments and DFT analysis.

Results and Discussion

Inspired by a manganese-catalyzed methodology for the reduction of quinolines reported by our group[26] and aiming to extend our recent efforts in using manganese catalysts for HIE,[27] we tested the reaction of various deuterium sources with quinoline with and without base in the presence of 10 mol% manganese pentacarbonyl bromide. Using DMSO-d_6 and KO*t*Bu, we were pleased to see that a significant amount of deuterium had been introduced into the substrate. Surprisingly, assignment of the NMR resonances using 2D NMR spectroscopy revealed that deuterium had been incorporated in positions 3 and 4, remote from the potentially coordinating nitrogen atom (Scheme 2). Intrigued by this selectivity, we performed control reactions in the absence of the manganese complex and found that the same result can be achieved with only base and deuterium source. A quick survey of the literature showed that the combination of KO*t*Bu and DMSO-d_6 had previously been used for the base-mediated deuteration of benzylic positions, although the pyridine and quinoline aromatic positions themselves remained largely unreactive towards isotopic exchange in the corresponding reports.[28] Other base-mediated HIE methodologies have targeted α-carbonyl positions or alkynes among others but have not been used on pyridines.[29] Encouraged by the complementarity of this reaction to other reports using the same deuteration system and to the existing strategies for the deuteration of azines, we decided to develop a general methodology for the remote deuteration of pyridine derivatives as well as bioactive molecules based on our findings.

To ensure a more general reaction and to allow for better comparison with a variety of previously reported methodologies, we used 2-phenylpyridine as model substrate for optimization. Under our initial reaction conditions and under an inert atmosphere, high deuterium incorporation was observed in distal positions 3, 4 and 5 (>80%), whereas only 23% of the hydrogen atom in α-nitrogen position 6 was exchanged and the phenyl ring remained untouched (Table 1, entry 1). This observed selectivity is remarkably different from previous HIE methodologies on pyridine substrates (*vide supra*). Deuterium incorporation for the targeted positions could be raised above 90% by using DMSO-d_6 as solvent (Table 1, entry 2) and selectivity was further improved by adding small amounts of water to the reaction mixture (Table 1, entry 3). This is probably due to the diminished overall basicity of the reaction mixture and the resulting slightly decreased reactivity. Lastly, it was found that reactivity was not impaired by increasing the scale of the reaction or by lowering the temperature to 90 °C (Table 1, entries 4 and 5). At the same time, the recovery of the deuterated product was slightly improved to 89% (Table 1, entry 4), hinting at a better chemoselectivity at lower temperature. Sequential deuteration of the isolated product could increase the deuterium content to 98% in the remote positions (entry 6), but a third run failed to raise the deuterium incorporation further (entry 7). Interestingly, the second and third deuteration cycle additionally resulted in an increased deuterium incorporation in the *ortho* positions of the phenyl

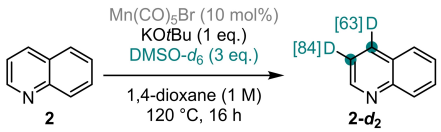

Scheme 2. Initial experiment: Remote deuteration of quinoline with KO*t*Bu and DMSO-d_6.

Research Article
doi.org/10.1002/ejoc.202200204

Chemistry Europe
European Chemical Societies Publishing

Table 1. Optimization of the deuteration of 2-phenylpyridine.

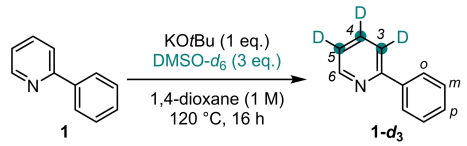

1 1-d_3

Entry[a]	Variation	D (3/4/5) [%][b]	D (6) [%]	D (*o*/*m*/*p*) [%]	yield [%][c]
1[d]	none	86	23	<10	83
2[e]	DMSO-d_6 as solvent (17 eq.)	96	20	13 (*o*)	82
3[d]	DMSO-d_6 as solvent, 1.1 eq. H_2O	95	14	<10	84
4[e]	DMSO-d_6 as solvent, 1.1 eq. H_2O, 90 °C	94	18	<10	89
5	DMSO-d_6 as solvent, 1.1 eq. H_2O, 90 °C, 5 mmol	95	11	<10	83
6	DMSO-d_6 as solvent, 1.1 eq. H_2O, 90 °C, 2nd cycle	98	12	15	n.d.
7	DMSO-d_6 as solvent, 1.1 eq. H_2O, 90 °C, 3rd cycle	98	13	20	n.d.
8	DMSO-d_6 as solvent, 1.1 eq. H_2O, 0.5 eq. KO*t*Bu	83	11	<10	n.d.
9	D_2O	<10	<10	<10	n.d.
10	Acetone-d_6	<10	<10	<10	n.d.
11	THF-d_8	<10	15	<10	n.d.
12	NaO*t*Bu, DMSO-d_6 as solvent, 90 °C	<10	<10	<10	n.d.
13	LiO*t*Bu	<10	<10	<10	n.d.
14	KOH, DMSO-d_6 as solvent, 90 °C	43[f], 70[g]	16	<10	n.d.
15	18-C-6 (1 eq.)	48	<10	<10	n.d.
16	*n*BuLi (1 eq.) and KO*t*Bu (1 eq.), dry DMSO-d_6 as solvent, rt	92[h], 66[i]	39	10	n.d.

[a] Scale: 0.5 mmol, work-up: extraction, then NMR in $CDCl_3$, deuterium incorporation was determined by ^{1}H NMR using the resonances of the non-deuterated *meta* and *para* positions in the phenyl substituent as a reference; [b] average; [c] isolated yield; [d] average of 2 runs; [e] average of 5 runs; [f] average of positions 3 and 5; [g] position 4; [h] average of positions 3 and 4; [i] position 5.

substituent. Overall, the reaction was very clean with small amounts (4% yield) of 2-phenyl-6-trideuteromethylpyridine being the only observed byproduct. Its formation likely stems from a competing Minisci-type radical trideuteromethylation as reported previously with DMSO-d_6.[30] Appreciable results could still be achieved with base loadings as low as 0.5 eq. (Table 1, entry 8). Interestingly, the reaction proved to be remarkably specific to both the deuterium source and the base: Other deuterium sources did not afford any isotopic exchange at all (Table 1, entries 9–11) and even simple replacement of KO*t*Bu by NaO*t*Bu or LiO*t*Bu completely shut down reactivity (Table 1, entries 12 and 13), whereas some reactivity was retained with KOH (Table 1, entry 14). Moreover, sequestration of potassium by addition of 18-C-6 significantly lowered the efficiency of the reaction (Table 1, entry 15), indicating that the cation plays a significant role in this transformation. When moving to Schlosser's base, the reaction could be carried out at room temperature, albeit with a different selectivity (Table 1, entry 16). Presumably, the reaction partially proceeds *via* dianions resulting from deprotonation of the *ortho*-metalated intermediate under these strongly basic conditions. This hypothesis would explain the higher amount of deuterium incorporation observed in position 6 compared to the reaction with KO*t*Bu as well as the reduced deuteration in position 5. The latter can be tentatively explained by the low stability of the vicinal dianion.

The reaction conditions explored above where applicable to a range of substituted pyridines and the selectivity pattern was maintained irrespective of the substitution sites (Scheme 3). High deuterium incorporation is usually obtained for the distal positions while deuteration in pyridine α-positions remained low. Concomitant deuteration was observed at more acidic sites such as in benzylic[28] (Scheme 3, compounds **5-d_4** and **8-d_4**) and α carbonyl (Scheme 3, compound **13-d_3**) positions as well as in a trifluoromethyl-substituted phenyl ring (Scheme 3, compound **3-d_6**). The reaction appeared to be somewhat sensitive to sterics and lower deuterium contents were measured in the proximity of larger aliphatic residues (Scheme 3, position 3 in compound **5-d_4**; positions 3 and 5 in compound **7-*d***). While the reactivity appears to be higher for electron-deficient substrates, for more electron-rich substrates a bias of the deuteration towards the *ortho* positions of electron-donating substituents could be observed, hinting at a change in mechanism in these cases (Scheme 3, compounds **9-d_2** and **10-*d***). High recoveries of the deuterated products were observed for pyridines exhibiting aromatic, aliphatic, trifluoromethyl, amide, as well as tertiary and free amine substituents, indicative of a good tolerance for these functional groups. However, halogenated substrates afforded a range of side products and therefore lower yields, presumably resulting from competing halogen transfer reactions under the basic reaction conditions.[31] Pyridines exhibiting cyano substituents, aldehyde moieties or terminal olefins and alkynes decomposed under the reaction conditions.

When moving beyond simple substituted pyridine derivatives, we were especially delighted to see that widely used ligands such as 2,6-bipyridine (Scheme 3, compound **17-d_7**), 1,10-phenanthroline (Scheme 3, compound **25-d_6**) and oxazolidinone **18-d_3** afforded high deuterium contents along with useful yields. Further, some bioactive molecules could be successfully labeled applying our methodology (Scheme 3, compounds **29**–**37**). For these molecules, deuterium was not only incorporated in heterocycles (Scheme 3, compounds **29-*d***, **30-*d***, **33-d_3**, **34-d_3**, **36-d_3**, **37-*d***) but also in chloro-substituted arenes (Scheme 3, **32-*d***, **34-d_{11}**, **35-d_4**) as previously reported for HIE reactions using KO*t*Bu and DMSO-d_6.[28b]

Having confirmed that the unusual remote deuteration pattern is consistently observed in the labeling reactions of several substrates, we became interested in understanding its origins. Initially, the fact that the reaction was significantly impaired when carried out at air (Table 2, entry 2) or in the presence of known radical scavengers such as (2,2,6,6-tetramethylpiperidin-1-yl)oxyl (TEMPO; Table 2, entry 3 and 4), *p*-benzoquinone (Table 2, entry 5) or butylated hydroxytoluene (BHT; Table 2, entry 6) led us to assume that free radicals could be involved in the reaction mechanism.[32] Besides, as no drastic differences were observed for the control reaction in the dark

Research Article
doi.org/10.1002/ejoc.202200204

Chemistry Europe
European Chemical Societies Publishing

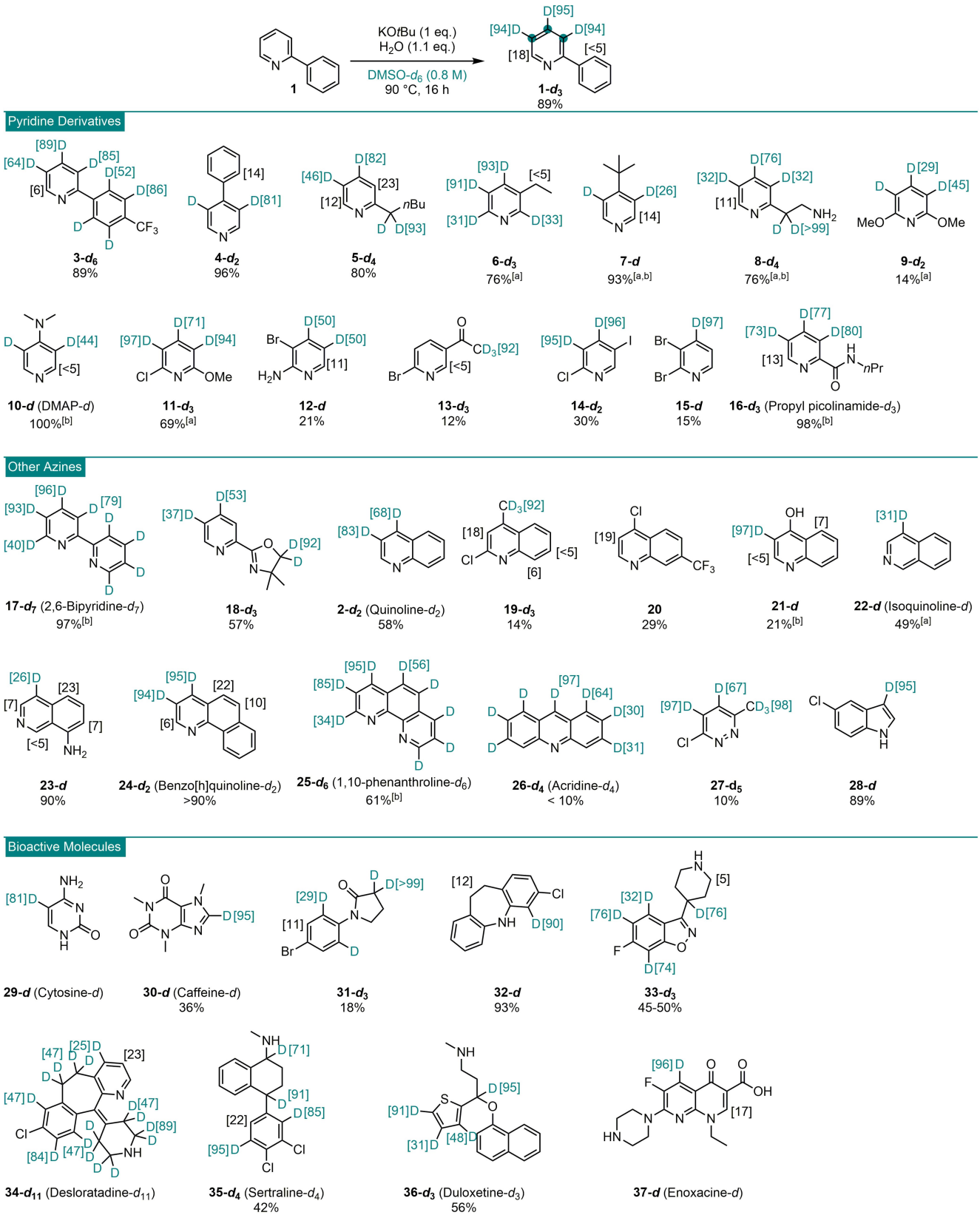

[a] Yield determined by NMR; [b] Reaction at 120 °C.

Scheme 3. Scope of the remote deuteration of pyridine derivatives.

Research Article
doi.org/10.1002/ejoc.202200204

Chemistry Europe
European Chemical Societies Publishing

Table 2. Effects of air and radical scavengers on the deuteration of pyridines.

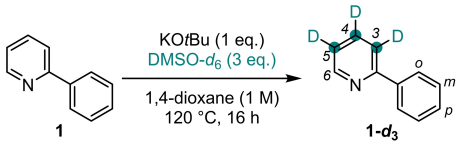

Entry[a]	Variation	D (3) [%]	D (4) [%]	D (5) [%]
1[b]	none	94	95	94
2	at air	2	11	6
3	TEMPO (1 eq.)	24	66	38
4	TEMPO (3 eq.)	15[c]	15[c]	16
5	*p*-benzoquinone (1 eq.)	1	1	1
6	BHT (1 eq.)	0	0	0
7	in the dark	66	94	84

[a] Scale: 0.5 mmol, crude NMRs were taken directly taken in the reaction solvent (DMSO-d_6), deuterium incorporation was determined by ^{1}H NMR using the resonances of the non-deuterated *meta* and *para* positions in the phenyl substituent as a reference. [b] Average of 5 runs. [c] Positions 3 and 4 are average values.

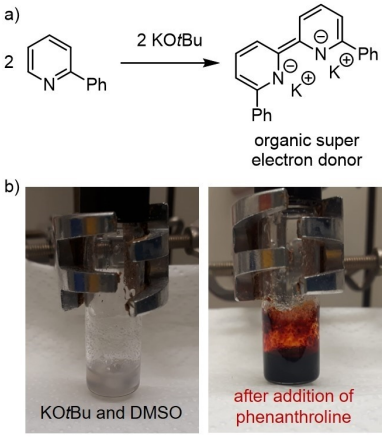

Scheme 4. a) Initially assumed formation of organic super electron donors from pyridine derivatives with KO*t*Bu. b) Color change observed after the addition of heteroarenes (in this case: 1,10-phenanthroline) to a solution of KO*t*Bu in DMSO-d_6.

(Table 2, entry 7), we reasoned that the reaction most likely proceeds by a ground-state pathway.

Given the rich literature precedence for this type of chemistry and its concordance with our results, we hypothesized that dimeric organic super electron donors might form from deprotonation of the substrate by KO*t*Bu (Scheme 4a).[33] They could then participate in single electron transfer (SET) pathways, thus kick-starting a radical chain reaction. In line with this hypothesis, we had observed intense color change when adding substrate to a solution of KO*t*Bu in DMSO-d_6 (Scheme 4b), indicative of the formation of conjugated dianionic species. Further, a similarly remarkable specificity for certain potassium-containing bases has been observed for previously reported reactions that proceed *via* the formation of organic super electron donors.

To further evaluate the possibility of a radical mechanism, we performed density functional theory (DFT) calculations and started by comparing the relative thermal stabilities of hypothesized intermediates to the observed selectivity. Based on previous theoretical studies,[34] we chose the M062X functional[35] with the 6-311+G(d,p) basis set for optimization in DMSO-d_6 solvent based on solute electron density (SMD).[36] Corrected Gibbs free energies at 298 K and 1 atm with solvation effect are used for our following discussions.

We computed the relative stability of all possible positional isomers of the radical species for 2-phenylpyridine (Figure 1). It was shown that the most stable radical isomer is at the **D6** position (−21.0 kJ/mol), followed by the *ortho* position (−5.7 kJ/mol) of the phenyl ring and the **D3** position (−1.6 kJ/mol) of the pyridine ring. The radical at the **D4** position (0.0 kJ/mol) as well as those at the *meta* and *para* positions (0.9 and 1.8 kJ/mol) are close in energy. The least stable radical is at the **D5** position (9.2 kJ/mol). Considering that the deuteration degree will follow the stability order of the radical species, the

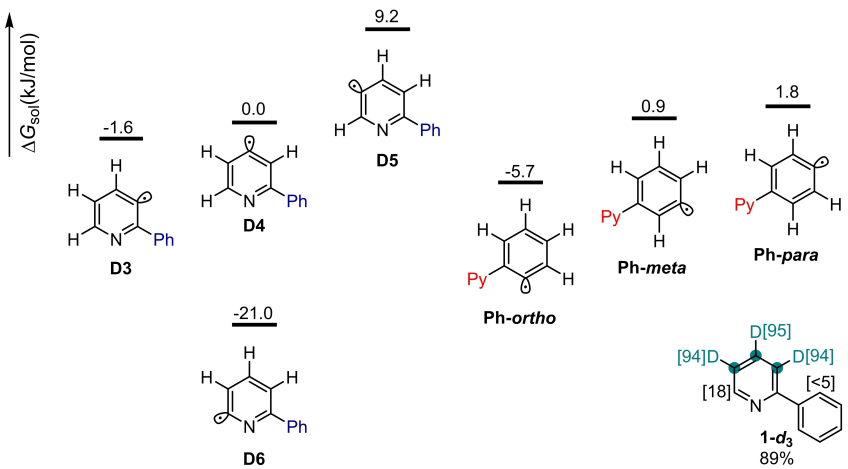

Figure 1. Relative Gibbs free energies of radical species of 2-phenylpyridine.

Research Article
doi.org/10.1002/ejoc.202200204

Chemistry Europe
European Chemical Societies Publishing

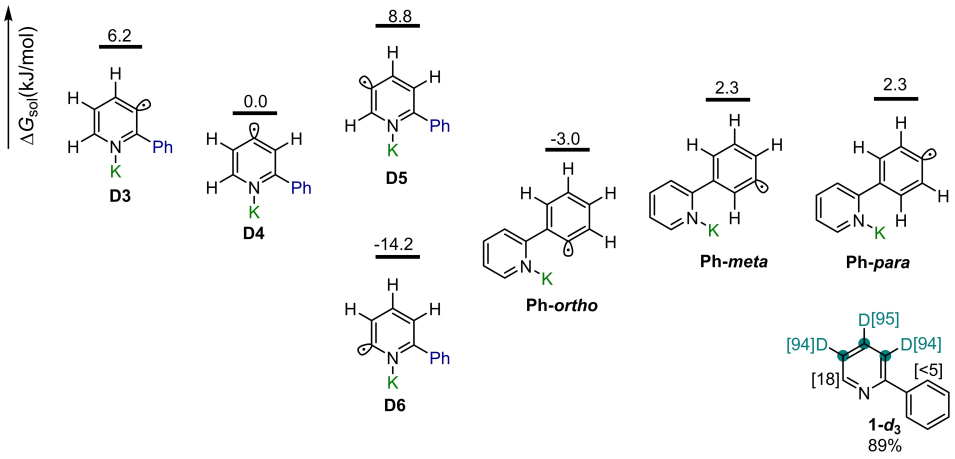

Figure 2. Relative Gibbs free energy of K^+ coordinated radical species of 2-phenylpyridine.

corresponding relative stability of these radical species does not agree with the deuteration distributions found experimentally.

In searching an alternative explanation for our experimentally observed selectivity, we explored the effect of potassium coordination on the stability of hypothesized radical intermediates. It was found that K^+ prefers coordinating with the nitrogen center instead of the radical center and the aromatic face site. As shown in Figure 2, the presence of K^+ changes the relative stability to some extent, however, it does not change the relative order; and the **D6** radical is still the most abundant intermediate.

Next, we briefly investigated steric effects from KO*t*Bu coordination to the pyridine nitrogen atom that could override thermodynamic preferences. However, we quickly discarded this hypothesis after observing a clear indication for a polar mechanism from additional experimental work for the analysis of linear free energy relationships with Hammett parameters. As shown in Figure 3, we found a very good correlation and a positive slope for Hammett σ and σ^- values with the relative initial reaction rates of substrates with various substituents at the *p*-position in the phenyl ring of 2-phenylpyridine, indicative of a transition state with a build-up of negative charge (Figure 3a and b), while only poor correlation was observed for radical $\sigma^{\cdot}$ parameters (Figure 3c).

In general, the combination of DMSO and KO*t*Bu is considered as a super-base system[37] and the corresponding anionic mechanism has been proposed.[28b] Thus, we calculated the relative Gibbs free energies of the anionic species of 2-phenylpyridine (Figure 4). Apparently, the stability of these anions can be divided into two groups, the more stable one including the **D3** (1.2 kJ/mol), **D4** (0.0 kJ/mol) and **D5** (2.8 kJ/mol) anions in very close energy; and the much less stable one including the **D6** anion (19.2 kJ/mol) as well as the *ortho*-, *meta*- and *para*-anions of the phenyl ring (13.1, 18.8 and 19.0 kJ/mol, respectively). This shows that deuteration at the 3, 4 and 5-positions of the pyridine ring should be most favored thermodynamically and deuteration at other positions is less likely. This agrees perfectly with our experimental observation, *i.e.*, 3-, 4 and 5-positions of the pyridine ring are nearly equally populated (94, 95 and 94 %, respectively). In addition, long time and sequential experimental results also show the possible deuteration at the D6 position as well as at the *ortho* position of the phenyl ring (Scheme 5). Remarkably, kinetic analysis revealed that the most stable anion is deuterated first (Scheme 5, position 4). Therefore, the anionic mechanism can explain the generation of the main product thermodynamically.

Considering the existence of potassium in the reaction system, we contemplated the effect of this cation on the stability of anions and the corresponding data is shown in Figure 5. The optimized structures show that the pyridine nitrogen atom interacts with K^+ for **D6** and **Ph-*ortho*** anions which increases the thermal stability. However, those more stable **D6** (−5.3 kJ/mol) and **Ph-*ortho*** (−6.8 kJ/mol) anions pose lower yield than less stable **D4** (0.0 kJ/mol) and **D5** (0.8 kJ/mol), so this mechanism is not consistent with "thermal selectivity". In summary, the coordination of K^+ can affect the relative stability

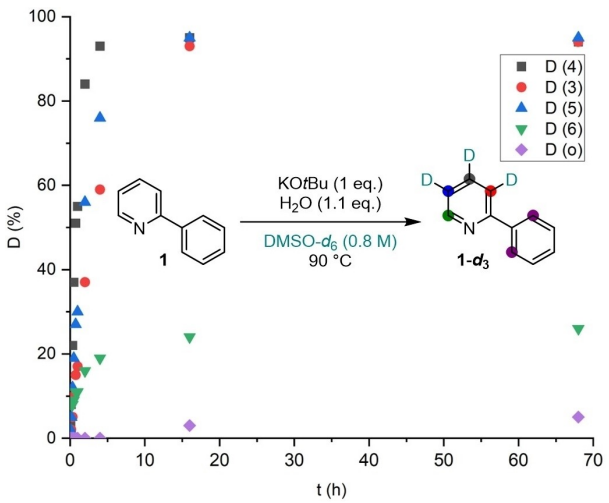

Scheme 5. Kinetic profile for the deuteration of 2-phenylpyridine.

Research Article
doi.org/10.1002/ejoc.202200204

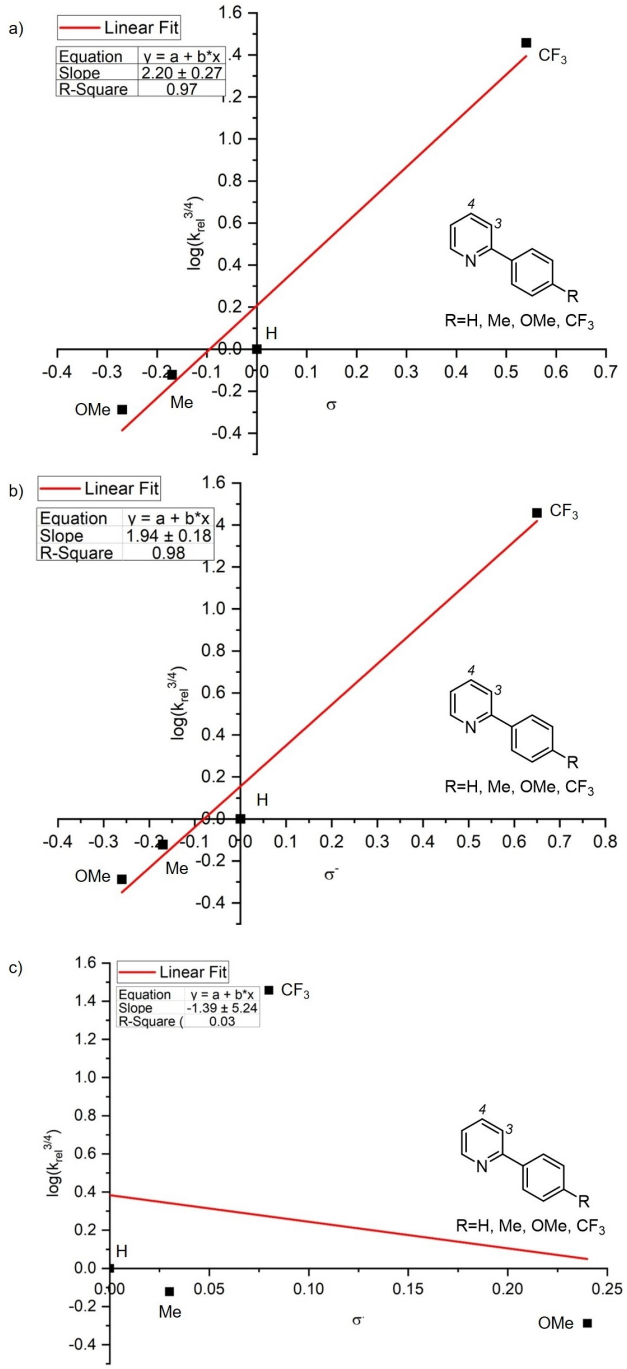

Figure 3. Hammett plots for the relative rates of deuteration in positions 3 and 4 for variously substituted 2-phenylpyridines a) with standard σ parameters, $R^2 = 0.97$; b) with σ^- parameters, $R^2 = 0.98$; c) with $\sigma^\cdot$ parameters, $R^2 = 0.03$.

of anions and there is no correlation between relative Gibbs free energy and deuteration yield. Therefore, this reaction mechanism is not possible thermodynamically.

From the above experimental and computational results, we know that the free anionic mechanism can account well for the deuteration preference in experiment for 2-phenylpyridine. The more thermally stable the pyridine ring anion, the higher the experimental deuterated yield. In addition, we computed the effect of pre-deuteration on the phenyl substituent (Table S13) and found that starting with **1-*d*$_1$**, **1-*d*$_2$** and **1-*d*$_3$**, the stability of the corresponding anions at the phenyl substituent does not change and the observed increase in the deuteration degree at the *ortho* position of the phenyl ring should be due to the excess of the deuterium source.

Furthermore, we found the relative deuterated yield for other pyridine derivatives, *N*,*N*-dimethylpyridin-4-amine, 4-(*tert*-butyl)pyridine, 2-(4-(trifluoromethyl)phenyl)pyridine, 2,2′-bipyridine, 4-chloro-7-(trifluoromethyl)quinoline, quinoline and phenanthroline, can also be consistent with an anionic mechanism (Figure S11.1–S11.7). Besides, excellent correlation between relative thermal stability of anionic species and deuteration yield are also found for other experimental results[25,28b] of the remote deuteration of pyridine derivatives, such as pyridine, 3,4-dimethylpyridine, 2,3-dimethylpyridine, 2-bromopyridine, 2-bromo-5-methylpyridine, 6-bromonicotinonitrile and 1-(difluoromethyl)-4-fluorobenzene (Figure S11.8–S11.14), as well as the deuteration of bioactive molecules in our own scope (caffeine, Figure S11.15). Using the anion stabilities, we have been able to successfully predict the order of deuterium incorporation in the different positions of new substrates (Scheme 6, Figure S11.16–S11.19). Although we have tried to explain and predict the deuteration yield on the basis of the ability of neutral substrates to generate anionic species, this has failed due to the different kinetic properties of different substrates.

Lastly, a measured KIE of 1.2 for positions 3 and 4 and 1.3 for position 5 hint at a reversible reaction. Since the KIE is small, the rate-determining step might not involve C–H cleavage at the substrate (Scheme 7). Rather, deuteration of the pyridyl anions or the generation of the dimsyl anion in the first place may represent the steps with the highest barriers.

Conclusion

In conclusion, we report a general and applicable base-mediated methodology for the remote deuteration of pyridine derivatives and other aromatic heterocycles with DMSO-d_6 as

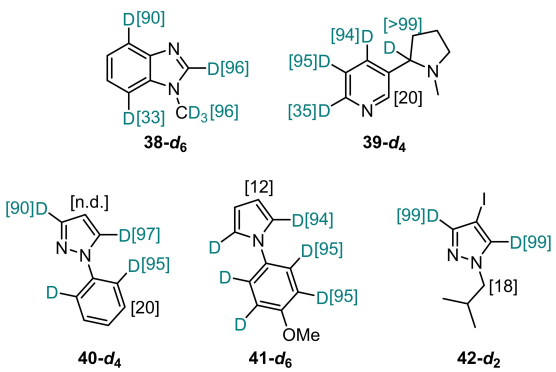

Scheme 6. Results of the deuteration reaction on substrates previously studied computationally.

Research Article
doi.org/10.1002/ejoc.202200204

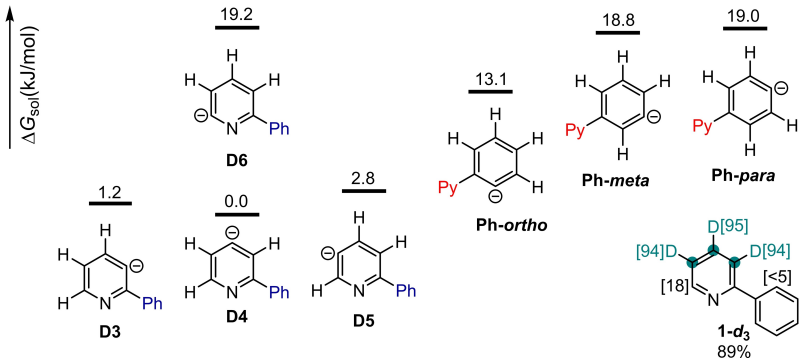

Figure 4. Relative Gibbs free energy of anionic species of 2-phenylpyridine.

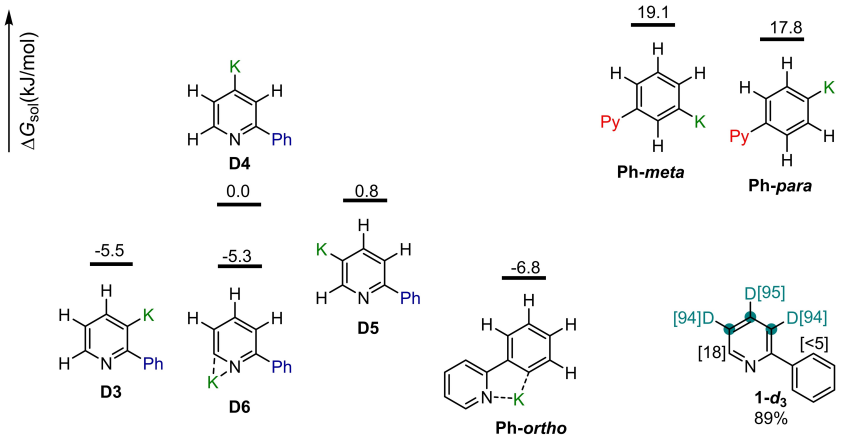

Figure 5. Relative Gibbs free energy of coordinated K^+ and anion species of 2-phenylpyridine.

deuterium source. Experimental and mechanistic studies including DFT calculations indicate that the reaction takes place *via* an anionic pathway and that thermodynamic stability of the respective anions corresponds well with the regioselectivity of deuteration. We have shown how these insights can be applied to predict the main deuteration sites of new substrates and we believe that these results will prove useful for the preparation of labeled MS standards and deuterated drugs. In a broader context, new transformations based on the generation of pyridyl anions by deprotonation with the dimsyl anion might be inspired by this report.

Experimental Section

General Deuteration Procedure: Potassium *tert*-butoxide (56 mg, 0.5 mmol, 1.0 eq.) and the substrate (if solid; 0.5 mmol) were weighed into a 25 mL pressure-resistant Schlenk tube equipped with a magnetic stirring bar. The Schlenk tube was capped with a rubber septum and evacuated and backfilled with argon three times. DMSO-d_6 (600 µL, 8.5 mmol, 17.0 eq.) was added followed by the substrate (if liquid; 0.5 mmol) and distilled water (10 µL, 5.6 mmol, 1.1 eq.). The Schlenk tube was closed, and the reaction mixture was subsequently heated to 90 °C and stirred at this temperature for 16 h. The resulting mixture was diluted with DCM, washed with brine (20 mL), and extracted with DCM (2×20 mL). The combined organic layers were dried over sodium sulfate and concentrated. Some compounds were sufficiently pure after extraction. The other deuterated products were purified by silica column chromatography.

Acknowledgements

We acknowledge the support from the European Union (Flow Chemistry for Isotope Exchange, FLIX, 862179), the BMBF and the State of Mecklenburg-Western Pommerania. We thank the analytical team of LIKAT for their kind support. J.L. thanks the European Union's Horizon 2020 research and innovation programme under the Marie Sklodowska-Curie grant agreement No. 859910. We thank Florian Bourriquen for insightful discussions. Open Access funding enabled and organized by Projekt DEAL.

Conflict of Interest

The authors declare no conflict of interest.

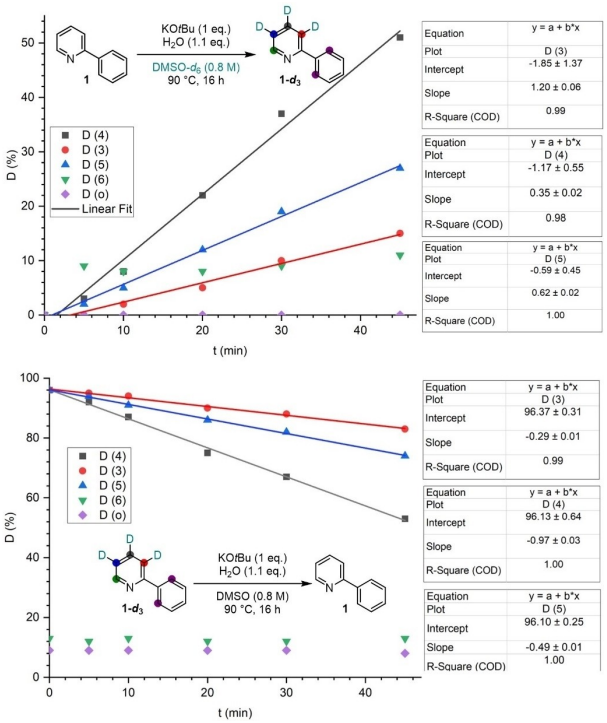

Scheme 7. Plots of initial velocities of the deuteration and the reverse reaction for the determination of kinetic isotope effects.

Data Availability Statement

The data that support the findings of this study are available in the supplementary material of this article.

Keywords: Density functional calculations · Deuterium · Heterocycles · Hydrogen isotope exchange · Isotopic labeling

[1] a) S. A. Blum, K. L. Tan, R. G. Bergman, *J. Org. Chem.* **2003**, *68*, 4127–4137; b) G. Lloyd-Jones, M. P. Muñoz, *J. Labelled Compd. Radiopharm.* **2007**, *50*, 1072–1087; c) M. Gómez-Gallego, M. A. Sierra, *Chem. Rev.* **2011**, *111*, 4857–4963; d) E. M. Simmons, J. F. Hartwig, *Angew. Chem. Int. Ed.* **2012**, *51*, 3066–3072; *Angew. Chem.* **2012**, *124*, 3120–3126; e) S. Kopf, F. Bourriquen, W. Li, H. Neumann, K. Junge, M. Beller, *Chem. Rev.* **2022**, *122*, 6634-6718.

[2] a) J. Atzrodt, V. Derdau, W. J. Kerr, M. Reid, *Angew. Chem. Int. Ed.* **2018**, *57*, 1758–1784; *Angew. Chem.* **2018**, *130*, 1774–1802; b) T. Pirali, M. Serafini, S. Cargnin, A. A. Genazzani, *J. Med. Chem.* **2019**, *62*, 5276–5297.

[3] J. Atzrodt, V. Derdau, W. J. Kerr, M. Reid, *Angew. Chem. Int. Ed.* **2018**, *57*, 3022–3047; *Angew. Chem.* **2018**, *130*, 3074–3101.

[4] E. Vitaku, D. T. Smith, J. T. Njardarson, *J. Med. Chem.* **2014**, *57*, 10257–10274.

[5] a) V. Marin, E. Holder, R. Hoogenboom, U. S. Schubert, *Chem. Soc. Rev.* **2007**, *36*, 618–635; b) B. Happ, A. Winter, M. D. Hager, U. S. Schubert, *Chem. Soc. Rev.* **2012**, *41*, 2222–2255; c) A. Gorczyński, J. M. Harrowfield, V. Patroniak, A. R. Stefankiewicz, *Chem. Rev.* **2016**, *116*, 14620–14674.

[6] a) G. Desimoni, G. Faita, P. Quadrelli, *Chem. Rev.* **2003**, *103*, 3119–3154; b) V. C. Gibson, C. Redshaw, C. A. Solan, *Chem. Rev.* **2007**, *107*, 1745–1776; c) J. I. van der Vlugt, J. N. H. Reek, *Angew. Chem. Int. Ed.* **2009**, *48*, 8832–8846; *Angew. Chem.* **2009**, *121*, 8990–9004; d) G. Yang, W. Zhang, *Chem. Soc. Rev.* **2018**, *47*, 1783–1810.

[7] a) J. B. Grimm, L. Xie, J. C. Casler, R. Patel, A. N. Tkachuk, N. Falco, H. Choi, J. Lippincott-Schwartz, T. A. Brown, B. S. Glick, Z. Liu, L. D. Davis, *JACS Au* **2021**, *1*, 690–696; b) H. J. Bae, J. S. Kim, A. Yakubovich, J. Jeong, S. Park, J. Chwae, S. Ishibe, Y. Jung, V. K. Rai, W.-J. Son, S. Kim, H. Choi, M. H. Baik, *Adv. Opt. Mater.* **2021**, *9*, 2170059.

[8] J. Chen, R. J. M. Klein Gebbink, *ACS Catal.* **2019**, *9*, 3564–3575.

[9] a) C. G. Macdonald, J. S. Shannon, *Tetrahedron Lett.* **1964**, *45*, 3351–3354; b) J. A. Zoltewicz, C. L. Smith, *J. Am. Chem. Soc.* **1966**, *88*, 4766–4767; c) J. A. Zoltewicz, C. L. Smith, *J. Am. Chem. Soc.* **1967**, *89*, 3358–3359; d) G. E. Calf, J. L. Garnett, V. A. Pickles, *Aust. J. Chem.* **1968**, *21*, 961–972; e) J. A. Zoltewicz, C. L. Smith, J. D. Meyer, *Tetrahedron* **1968**, *24*, 2269–2274 .

[10] a) X. Wang, M.-H. Zhu, D. P. Schuman, D. Zhong, W.-Y. Wang, L.-Y. Wu, W. Liu, B. M. Stoltz, W.-B. Liu, *J. Am. Chem. Soc.* **2018**, *140*, 10970–10974; b) C. Liu, S. Han, M. Li, X. Chong, B. Zhang, *Angew. Chem. Int. Ed.* **2020**, *59*, 18527–18531; *Angew. Chem.* **2020**, *132*, 18685–18689; c) W. Li, R. Qu, W. Liu, F. Bourriquen, S. Bartling, N. Rockstroh, K. Junge, M. Beller, *Chem. Sci.* **2021**, *12*, 14033–14038; d) Y. Li, Z. Ye, Y.-M. Lin, Y. Liu, Y. Zhang, L. Gong, *Nat. Commun.* **2021**, *12*, 2894–2906.

[11] a) N. Plé, A. Turck, K. Couture, G. Quéguiner, *J. Org. Chem.* **1995**, *60*, 3781–3786; b) P. Pierrat, P. Gros, Y. Fort, *Synlett* **2004**, *13*, 2319–2322; c) J. Hawad, O. Bayh, C. Hoarau, F. Trécourt, G. Quéguiner, F. Marsais, *Tetrahedron* **2008**, *64*, 3236–3245.

[12] a) J. A. Brown, S. Irvine, A. R. Kennedy, W. J. Kerr, S. Andersson, G. N. Nilsson, *Chem. Commun.* **2008**, 1115–1117 ; b) J. A. Brown, A. R. Cochrane, S. Irvine, W. J. Kerr, B. Mondal, J. A. Parkinson, L. C. Paterson, M. Reid, T. Tuttle, S. Andersson, G. N. Nilsson, *Adv. Synth. Catal.* **2014**, *356*, 3551–3562; c) M. Parmentier, T. Hartung, A. Pfaltz, D. Muri, *Chem. Eur. J.* **2014**, *20*, 11496–11504; d) K. Jess, V. Derdau, R. Weck, J. Atzrodt, M. Freytag, P. G. Jones, M. Tamm, *Adv. Synth. Catal.* **2017**, *359*, 629–638.

[13] M. Liu, X. Chen, T. Chen, S.-F. Yin, *Org. Biomol. Chem.* **2017**, *15*, 2507–2511.

[14] a) N. H. Werstiuk, C. Ju, *Can. J. Chem.* **1989**, *67*, 5–10; b) J. Yao, R. F. Evilia, *J. Am. Chem. Soc.* **1994**, *116*, 11229–11233.

[15] a) H. Esaki, N. Ito, S. Sakai, T. Maegawa, Y. Monguchi, H. Sajiki, *Tetrahedron* **2006**, *62*, 10954–10961; b) V. Derdau, J. Atzrodt, J. Zimmermann, C. Kroll, F. Brückner, *Chem. Eur. J.* **2009**, *15*, 10397–10404.

[16] V. H. Mai, O. B. Gadzhiev, S. K. Ignatov, G. I. Nikonov, *Catal. Sci. Technol.* **2019**, *9*, 3398–3407.

[17] a) C. G. Macdonald, J. S. Shannon, *Tetrahedron Lett.* **1964**, *45*, 3351–3354; b) G. E. Calf, J. L. Garnett, V. A. Pickles, *Aust. J. Chem.* **1968**, *21*, 961–972; c) R. B. Moyes, P. B. Welles, *J. Catal.* **1971**, *21*, 86–92; d) G. M. Rubottom, E. J. Evain, *Tetrahedron* **1990**, *46*, 5055–5064; e) E. Alexis, J. R. Jones, W. J. S. Lockley, *Tetrahedron Lett.* **2006**, *47*, 5022–5028; f) J. A. Sullivan, K. A. Flanagan, H. Hain, *Catal. Today* **2008**, *139*, 154–160; g) S. C. Schou, *J. Labelled Compd. Radiopharm.* **2009**, *52*, 376–381; h) K. R. Guy, J. R. Shapley, *Organometallics* **2009**, *28*, 4020–4027; i) D. Bouzouita, J. M. Asensio, V. Pfeifer, A. Palazzolo, P. Lecante, G. Pieters, S. Feuillastre, S. Tricard, B. Chaudret, *Nanoscale* **2020**, *12*, 15736–15742.

[18] G. Pieters, C. Taglang, E. Bonnefille, T. Gutmann, C. Puente, J.-C. Berthet, C. Dugave, B. Chaudret, S. Rousseau, *Angew. Chem. Int. Ed.* **2014**, *53*, 230–234; *Angew. Chem.* **2014**, *126*, 234–238.

[19] a) B. Gröll, M. Schnürch, M. D. Mihovilovic, *J. Org. Chem.* **2012**, *77*, 4432–4437; b) H. Yang, C. Zarate, W. N. Palmer, N. Rivera, D. Hesk, P. J. Chirik, *ACS Catal.* **2018**, *8*, 10210–10218; c) C. Zarate, H. Yang, M. J. Bezdek, D. Hesk, P. J. Chirik, *J. Am. Chem. Soc.* **2019**, *141*, 5034–5044.

[20] M. Daniel-Bertrand, S. Garcia-Argote, A. Palazzolo, I. M. Marin, P.-F. Fazzini, S. Tricard, B. Chaudret, V. Derdau, S. Feuillastre, G. Pieters, *Angew. Chem. Int. Ed.* **2020**, *59*, 21114–21120; *Angew. Chem.* **2020**, *132*, 21300–21306.

[21] R. P. Yu, D. Hesk, N. Rivera, I. Pelczer, P. J. Chirik, *Nature* **2016**, *529*, 195–199.

[22] J. L. Koniarczyk, D. Hesk, A. Overgard, I. W. Davies, A. McNally, *J. Am. Chem. Soc.* **2018**, *140*, 1990–1993.

[23] B. Eguillor, M. A. Esteruelas, J. García-Raboso, M. Oliván, E. Oñate, *Organometallics* **2009**, *28*, 3700–3709.

[24] J. A. Zoltewicz, C. L. Smith, *J. Am. Chem. Soc.* **1967**, *89*, 3358–3359.

[25] Y. Li, C. Zheng, Z.-J. Jiang, J. Tang, B. Tang, Z. Gao, *Chem. Commun.* **2022**, *58*, 3497–3500.

[26] V. Papa, Y. Cao, A. Spannenberg, K. Junge, M. Beller, *Nat. Catal.* **2020**, *3*, 135–142.

[27] S. Kopf, H. Neumann, M. Beller, *Chem. Commun.* **2021**, *57*, 1137–1140.

[28] a) Y. Hu, L. Liang, W.-T. Wei, X. Sun, X.-J. Zhang, M. Yan, *Tetrahedron* **2015**, *71*, 1425–1430; b) L. Huang, W. Liu, L.-L. Zhao, Z. Zhang, X. Yan, *J. Org. Chem.* **2021**, *86*, 3981–3988.

[29] a) S. P. Bew, G. D. Hiatt-Gipson, J. A. Lovell, C. Poullain, *Org. Lett.* **2012**, *14*, 456–459; b) M. Zanatta, F. P. dos Santos, C. Biehl, G. Marin, G. Ebeling, P. A. Netz, J. Dupont, *J. Org. Chem.* **2017**, *82*, 2622–2629; c) T. R.

Puleo, A. J. Strong, J. S. Bandar, *J. Am. Chem. Soc.* **2019**, *141*, 1467–1472; d) V. Salamanca, A. C. Albéniz, *Eur. J. Org. Chem.* **2020**, 3206–3212; e) K. I. Galkin, E. G. Gordeev, V. P. Ananikov, *Adv. Synth. Catal.* **2021**, *363*, 1368–1378.

[30] a) R. Caporaso, S. Manna, S. Zinken, A. R. Kochnev, E. R. Lukyanenko, A. V. Kurkin, A. P. Antonchick, *Chem. Commun.* **2016**, *52*, 12486–12489; b) R. Zhang, X. Shi, Q. Yan, Z. Li, Z. Wang, H. Yu, X. Wang, J. Qi, M. Jiang, *RSC Adv.* **2017**, *7*, 38830–38833; c) R. A. Garza-Sanchez, T. Patra, A. Tlahuext-Aca, F. Strieth-Kalkhoff, F. Glorius, *Chem. Eur. J.* **2018**, *24*, 10064–10068.

[31] a) A. Vaitiekunas, F. F. Nord, *Nature* **1951**, *168*, 875–876; b) M. Schnürch, M. Spina, A. F. Khan, M. D. Mihovilovic, P. Stanetty, *Chem. Soc. Rev.* **2007**, *36*, 1046–1057; c) T. R. Puleo, D. R. Klaus, J. S. Bandar, *J. Am. Chem. Soc.* **2021**, *143*, 12480–12486.

[32] C. L. Øpstad, T.-B. Melø, H.-R. Sliwka, V. Partali, *Tetrahedron* **2009**, *65*, 7616–7619.

[33] a) S. Yanagisawa, K. Ueda, T. Taniguchi, K. Itami, *Org. Lett.* **2008**, *10*, 4673–4676; b) W. Liu, H. Cao, H. Zhang, H. Zhang, K. H. Chung, C. He, H. Wang, F. Y. Kwong, A. Lei, *J. Am. Chem. Soc.* **2010**, *132*, 16737–16740; c) E. Shirakawa, K.-I. Itoh, T. Higashino, T. Hayashi, *J. Am. Chem. Soc.* **2010**, *132*, 15537–15539; d) A. Studer, D. P. Curran, *Angew. Chem. Int. Ed.* **2011**, *50*, 5018–5022; *Angew. Chem.* **2011**, *123*, 5122–5127; e) E. Shirakawa, T. Hayashi, *Chem. Lett.* **2012**, *41*, 130–134; f) S. Zhou, G. M. Anderson, B. Mondal, E. Doni, V. Ironmonger, M. Kranz, T. Tuttle, J. A. Murphy, *Chem. Sci.* **2014**, *5*, 476–482; g) J. P. Barham, G. Coulthard, R. G. Kane, N. Delgado, M. P. John, J. A. Murphy, *Angew. Chem. Int. Ed.* **2016**, *55*, 4492–4496; *Angew. Chem.* **2016**, *128*, 14568–4572; h) J. P. Barham, G. Coulthard, K. J. Emery, E. Doni, F. Cumine, G. Nocera, M. P. John, L. E. A. Berlouis, T. McGuire, T. Tuttle, J. A. Murphy, *J. Am. Chem. Soc.* **2016**, *138*, 7402–7410; i) L. Zhang, H. Yang, L. Jiao, *J. Am. Chem. Soc.* **2016**, *138*, 7151–7160; j) M. Patil, *J. Org. Chem.* **2016**, *81*, 632–639; k) J. Madasu, S. Shinde, R. Das, S. Patel, A. Shard, *Org. Biomol. Chem.* **2020**, *18*, 8346–8365.

[34] a) L. Zhang, H. Yang, L. Jiao, *J. Am. Chem. Soc.* **2016**, *138*, 7151–7160; b) W.-B. Liu, D. P. Schuman, Y.-F. Yang, A. A. Toutov, Y. Liang, H. F. T. Klare, N. Nesnas, M. Oestreich, D. G. Blackmond, S. C. Virgil, S. Banerjee, R. N. Zare, R. H. Grubbs, K. N. Houk, B. M. Stoltz, *J. Am. Chem. Soc.* **2017**, *139*, 6867–6879; c) S. Banerjee, Y.-F. Yang, I. D. Jenkins, Y. Liang, A. A. Toutov, W.-B. Liu, D. P. Schuman, R. H. Grubbs, B. M. Stoltz, E. H. Krenske, K. N. Houk, R. N. Zare, *J. Am. Chem. Soc.* **2017**, *139*, 6880–6887.

[35] Y. Zhao, D. G. Truhlar, *Theor. Chem. Acc.* **2008**, *120*, 215–241.

[36] A. V. Marenich, C. J. Cramer, D. G. Truhlar, *J. Phys. Chem. B* **2009**, *113*, 6378–6396.

[37] B. A. Trofimov, E. Y. Schmidt, *Acc. Chem. Res.* **2018**, *51*, 1117–1130.

Manuscript received: February 22, 2022
Revised manuscript received: March 14, 2022
Accepted manuscript online: March 15, 2022